

GROUND DEFORMATION DETECTION ALONG THE QINGHAI-TIBET RAILWAY

W. Y. Gong *, J. X. Zhang, Y. H. Zhang

Chinese Academy of Surveying and Mapping, 100039 Haidian, Beijing - (gongwy,zhangjx, yhzhang)@casm.ac.cn

KEYWORDS: Image Processing, Earth Deformation, Interferometric SAR (InSAR), Change Detection, Ground Deformation Hazard Mitigation

ABSTRACT:

In this contribution, we focus on the ground deformation along the Qinghai-Tibet Railway based on the InSAR technique. Qinghai-Tibet Railway, the highest railway in the world, stretches 1,956 kilometres from Xining to Lhasa cities in western China. It lies on the Tibetan Plateau where the geological structural is extremely complex. And it goes through twelve regional seismotectonic zones where some great earthquakes had occurred. Consequently, we need to find out the ground deformation along the Qinghai-Tibet Railway. We have chosen a typical area located at the west of the Kunlun Mountains nearby a part of the railway where the main land cover types are meadow, lake and mountain. The Persistent Scatterer technique has been introduced in our experiment. It can be used to generate precise ground deformation in our study area. It aims at separating the phase terms (possible target motion, atmospheric phase contribution, decorrelation noise, residual topographic phase) by exploiting their different spectral behavior in the framework of a multi-dimensional joint analysis. The best place to use the PS approach is within urban area. Nevertheless, our researches have proven the probability to use PS technique in the Tibetan Plateau earthquake monitoring.

1. INTRODUCTION

1.1 Study Area

Qinghai-Tibet Railway, the highest railway in the world, stretches 1,956 kilometers from Xining to Lhasa cities in western China. It lies on the Tibetan Plateau where the geological structural is extremely complex. It goes through twelve regional seismotectonic zones where had occurred some great earthquakes (e.g., there was an earthquake of magnitude 8.1 in the west to Kunlun Mountain on November 11th 2001). Previous research on these zones had proved that the active faults which have strike slip rate of 4-15 mm per year are possible to trigger strong earthquakes of $M_s \geq 6-7$. This factor and other hazard effects lead to ground deformation, which endanger the safety of the Qinghai-Tibet Railway. The coupling of the railway and active faulting has a higher hazard to occur the ground deformation.

On the other hand, such huge project in Tibet Plateau will certainly lead to some geologic influence that is still waiting for our investigation. Such research is quite important for the disaster forecast and environment protection. Therefore, we need to find out the ground deformation along the Qinghai-Tibet Railway.

Interferometric synthetic aperture radar (InSAR) has proven capable of mapping ground deformation with centimeter-scale precision and producing accurate DEMs with several meters accuracy (Lu, 2003), and the ground coverage of thousands of square kilometers per image scene.

The center latitude of the study area is 35.79 degrees and the longitude is 93.422. It is located at the west of part of the Qinghai-Tibet rail way not very far from the Kunlun Mountains (Fig.1).

The images of the study is seven segment of the ENVISAT image, which is 600 pixel \times 600 pixel large. The resolution of the image is 15m in the range and 40m in the azimuth.

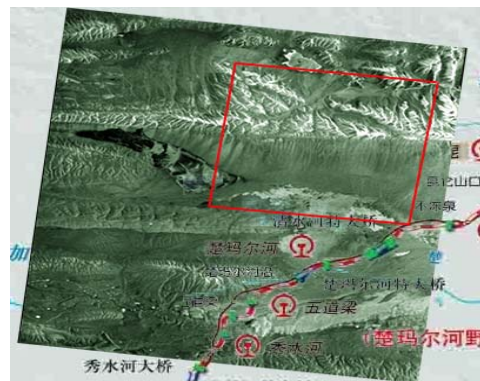


Figure 1. Study area (Our study area is part of the acquired SAR image near the rail way)

1.2 General Method of Research

In this paper, we use InSAR-derived DEMs to estimate the deformation in the study areas. PS is a proper approach to the time series deformation detection, which could deal with the weakness of the traditional Differential InSAR processing. The permanent scatterers of the study area may much less than in the city region. The most of them may be nature's structures, and they are found either in coherent and non-coherent areas. However, the stack of image isn't big enough so that we have to do phase unwrapping before the phase model refinement.

* Corresponding author Wenyu Gong. Chinese Academy of Surveying and Mapping, 100039 Beitaping Road, Haidian, Beijing - gongwy@casm.ac.cn

Finally, the displacement map of the PS targets can be reconstructed.

2. DEM GENERATION

The main interferometric processing steps include SAR image o-registration, formation of interferogram, and separation of deformation information, phase unwrapping and geocoding (Guoxiang. Liu, 2006). The theory of DEM reconstruction processing has been addressed in many papers. Here we just review the key step of it.

The first step was the selection of SAR images to generate the interferogram. SAR images acquired. The interval time of the pair we used to generate the DEM is about 210 days.

The second step is SAR image co-registration and resampling. Co-registration is the process of lining up two images, namely the master and the slave image covering the same region During the InSAR processing; co-registration of imagery has been a key pre-requisite for the following procedures. In order to do an exact alignment, one first has to determine matching polynomials with which the slave image is shifted and rotated to fit closest to the master image. The method we used to estimate matching model is based on the image intensity. It does not depend on the level of coherence between the two SLC and is computational efficient. And it requires at least a minimum of image contrast. After SAR image co-registration, it is very important to correctly resample the slave image into the master image grid using the refined co-registration model.

Then the formation of an interferogram performed by pixel multiplication between two SAR images. Once the complex wrapped image is obtained, the flat-earth trend was removed.

The third step was phase unwrapping. Phase filtering is performed in order to overcome the problems of phase noise before unwrapping. It is then done by the method uses minimum cost flow (MCF) and a triangular irregular network (TIN), which is a global optimization technique to the phase unwrapping problem. The gaps (e.g. at locations of very low coherence) in the input data can be considered and the higher density of the triangular network.

The last step is height map generation. For the prior research has proven that the orbit error always leads to inexact result. The DELFT precision orbit state vectors data was used to achieve a good baseline estimate. We used the phase unwrapped interferogram and the baseline geometry to reconstructs the terrain height.

3. PS PROCESSING

Differential Interferometric synthetic aperture radar has proven a remarkable potential for mapping ground deformation phenomena With the information-derived form the interferometric data sets, the accuracy of deformation can be min-meter level detected with D-InSAR. However there are some disadvantages such as decorrelation and atmosphere contribution. The PS processing is one of the ways that can overcome the weakness of the DInSAR processing and deliver the more precision result.

The Permanent Scatterer (PS) technique has been developed by A.Ferretti, F. Rocca, and C. Prati of the Technical University of Milan (POLIMI) in the late 1990s to overcome the major limitations of D-InSAR processing, temporal and geometrical decorrelation, and variations in atmospheric conditions.

3.1 Pre-processing

In our experiment, Seven ENVISAT SAR image were used to perform PS processing. The first image was date on August 5th 2003, and the last one on 28th 2006, as the Fig 2 shows. The image acquired at Jun 1st 2006 was chosen as master image and the others were the reference image. Master image was selected by the following criteria.

1. Doppler centroid near average Doppler Centroid of considered SAR acquisitions
2. Orbit near geometric centre of orbit tube spanned by available SAR acquisitions
3. Low atmospheric distortions
4. Acquisition date near temporal average of available
5. SAR acquisitions

The largest perpendicular baseline is about 1338.81m and the longest time interval is 875 days

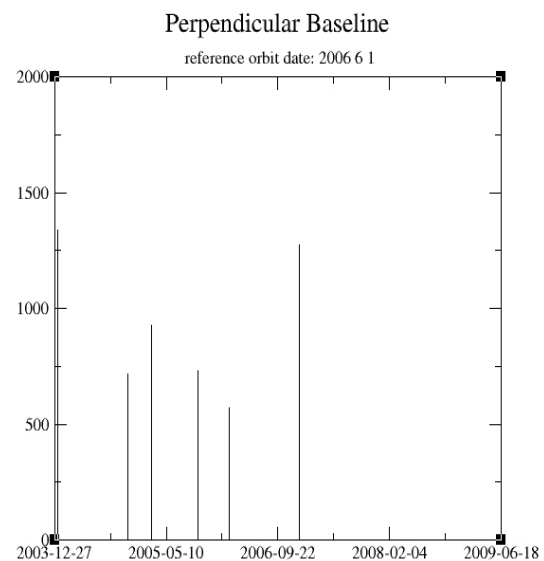


Figure 2. Perpendicular baseline components relative to the selected reference orbit 1-June-2006

A selection of PS based on the coherence and an additional dominant backscattering is used. About 20305 PS candidates (PSC) were found (Fig.3).

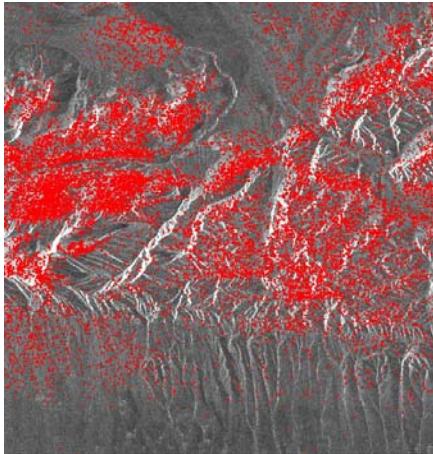


Figure 3. Persistent Scatterer Candidates (red points)

3.2 Phase Model Construction and Analysis

After we used InSAR-derived DEM to removing the topographic, the differential phase of each PS can be expressed as follows

$$\varphi_i = K_1 \cdot B_i \cdot \xi_h + K_2 \cdot T_i \cdot v + \varphi_{res}$$

Where φ_i is the phase associated with differential interferogram i , K_i are constants, B_i are perpendicular baseline, T_i are the temporal baseline, ξ_h are the DEM residual error, V are the deformation velocity, and φ_{res} are the non-linear terms related with atmospheric variances and non-linear velocity components.

For the small data stack (less than 30 SAR image), spatial phase unwrapping is required prior to the regression step. A phase unwrapping method based on Minimum Cost Flow optimization techniques applied to a triangular irregular network is used in our study (Fig 4).

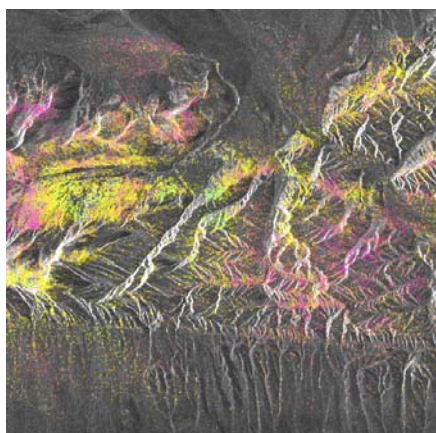


Figure 4. The phase of the PSC after unwrapping

The following PS procedure to do model refinement is based on a non-linear least squares error analysis by which we can calculate the displacement velocity, atmosphere contribution, DEM residual error and non-linear displacement velocity of the study areas. A flow chart of our PS processing sequence is shown in Figure 5.

Accompany the processing, the quality measure for the phase standard deviation (sigma) of the PSC is calculated. This factor includes terms related to phase noise, atmospheric path delay related phase, deformation phase, and baseline error related phase. The one with too big sigma were rejected, while the others are used to update the model.

At last, on 2329 PS were used to do model refinement. The results from the model analysis are height corrections, linear deformation rates, a quality measure, and residual phases.

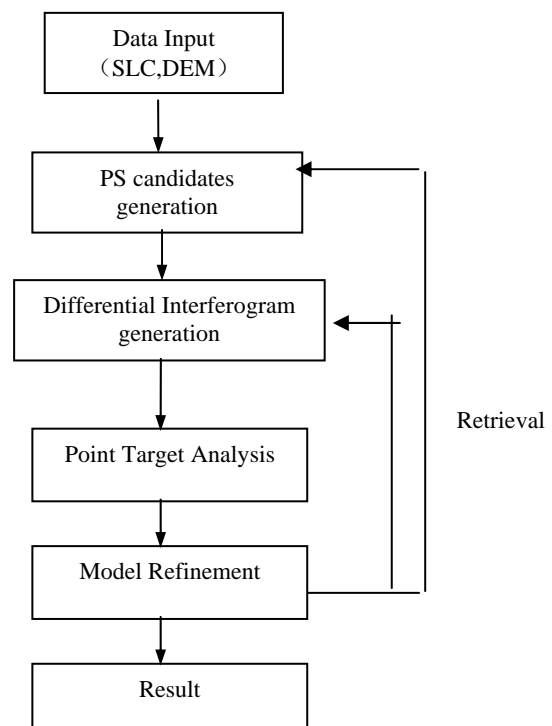


Figure 5. PS Processing Flow Chart

3.3 Estimation of atmospheric phases and non-linear velocity

The atmospheric path delay is low-pass in the spatial dimension, but uncorrelated from pass to pass. The non-linear deformation is generally low-pass in the spatial and temporal dimension. These two contributions were separated from the residual phase by filtering.

3.4 Result of the experiment

In Fig.6, the deformation level of the PS is shown. For the large majority of the points the deformation rate estimated is below 1mm/year.

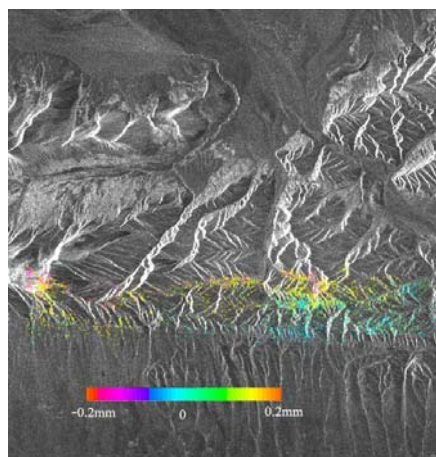


Figure 6 Deformation Levels of the 2329 PS Targets (2004-2006)

We expanded the existing solution to additional points by interpolation (Fig 7).

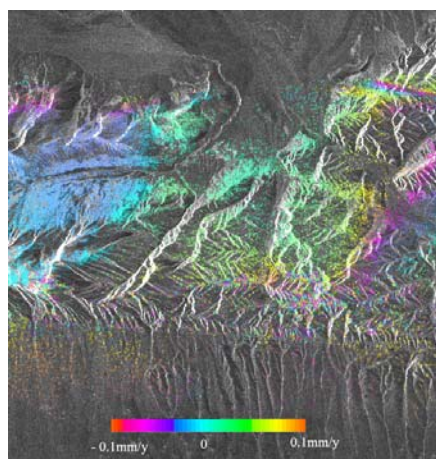


Figure 7 Linear Deformation velocity of the all PSC (after interpolation)

4. CONCLUSION

Using the PS technique, we computed out the deformation level of the study area between the 2004-2006 with the InSAR generated DEM. The deformation rate of the 2329 PS targets are achieved. The velocity of the majority of them is below the 0.1mm/year (Fig.7). During the processing, the single coherent pixel can be identified. In the large temporal and geometric baselines, only point wise targets carry targets carry useful phase information. In our experiment, the largest perpendicular baseline is 1338.81m (the limitation of the DInSAR is about less than 1200m).

Most of the experiments of the PS technique were done in the urban region. Because of the PS targets is quite rare in the rural region. In our study, the PS is almost rockies around the mountains. For Tibet area, the PS targets is much less than the other place. The winter is lasted about half of the yearlong. So

the thick snow hat of the study area is one of the big problems for PS processing.

Our study shows the probability of the PS processing in the rural region. While, the precision ground surveying data is invalid during our experiment. The more study should be done in order to confirm the results. Another remark is that for more than 30 SAR images, the step of unwrapping and model refinement could be done together that can remove the error from the incorrect phase unwrapping.

ACKNOWLEDGEMENTS

This work is support by National Key Basic Research and Development Program (973 program) under Grant No.2006CB701303. The SAR data is provided by ESA through Dragon Program with ID 4803

REFERENCE

- Bert M.Kampes, 2006, *Radar Interferometry----Persistent Scatterer Techninque*, Springer, The Netherlands
- Colesanti, C., et al., 2003, SAR monitoring of progressive and seasonal ground deformation using the permanent scatterers technique, *IEEE Transactions on Geoscience and Remote Sensing*, 41(7), pp. 1685-1701.
- Ferretti, A., 2000a, Nonlinear subsidence rate estimation using permanent scatterers in differential SAR interferometry, *IEEE Transactions on Geoscience and Remote Sensing*, 38(5), pp. 2202-2212.
- Ferretti, A., 2001b, Permanent scatterers in SAR interferometry, *IEEE Transactions on Geoscience and Remote Sensing*, 39(1), pp. 8-20.
- Guoxiang, L 2006, *Monitoring of Ground Deformations with Radar Interferometry*, China Map Publishing Company, Beijing.
- Hanssen,,R.F., 2001, *Radar Interferometry----Data Interpretation and Error Analysis*, Kluwer Academic Publisher, The Netherlands
- Lu, Z., 2000, Synthetic Aperture Radar interferometry of Okmok volcano, Alaska: Radar observations, *Journal of Geophysical Research*, 105(B5), pp. 10791-10806.

DEFLT orbit precision states vectors, Delft University of Technology: <http://enterprise.lr.tudelft.nl>.